



Crystal structure of the RNA demethylase ALKBH5 from zebrafish



Weizhong Chen^{a,b,c}, Liang Zhang^b, Guanqun Zheng^b, Ye Fu^b, Quanjiang Ji^b, Fange Liu^b, Hao Chen^c, Chuan He^{b,*}

^a Department of Chemical Physics, University of Science and Technology of China, Hefei, Anhui 230026, China

^b Department of Chemistry and Institute for Biophysical Dynamics, The University of Chicago, 929 E. 57th Street, Chicago, IL 60637, USA

^c Coordination Chemistry Institute and the State Key Laboratory of Coordination Chemistry, School of Chemistry and Chemical Engineering, Nanjing University, Nanjing 210093, China

ARTICLE INFO

Article history:

Received 23 December 2013

Revised 27 January 2014

Accepted 8 February 2014

Available online 20 February 2014

Edited by Christian Griesinger

Keywords:

ALKBH5

Crystal structure

Demethylation

N⁶-Hydroxymethyladenosine

ABSTRACT

ALKBH5, a member of AlkB family proteins, has been reported as a mammalian N⁶-methyladenosine (m⁶A) RNA demethylase. Here we report the crystal structure of zebrafish ALKBH5 (fALKBH5) with the resolution of 1.65 Å. Structural superimposition shows that fALKBH5 is comprised of a conserved jelly-roll motif. However, it possesses a loop that interferes potential binding of a duplex nucleic acid substrate, suggesting an important role in substrate selection. In addition, several active site residues are different between the two known m⁶A RNA demethylases, ALKBH5 and FTO, which may result in their slightly different pathways of m⁶A demethylation.

Structured summary of protein interactions:

ALKBH5 and **ALKBH5** bind by x-ray crystallography (View interaction)

© 2014 Federation of European Biochemical Societies. Published by Elsevier B.V. All rights reserved.

1. Introduction

Among the various RNA modifications, N⁶-methyladenosine (m⁶A) is of great interest because it is the most prevalent internal modification in eukaryotic mRNA [1]. This modification also exists in the virus RNA that is transcribed in host nuclei [2], and plays an important role in yeast meiosis and plant development [3,4]. An RNA methyltransferase complex with METTL3 as one of the S-adenosylmethionine-binding subunit installs the N⁶-position methyl group of m⁶A [5]. Our recent discoveries of two m⁶A demethylases (FTO and ALKBH5) specifically highlight the importance of the reversal of this modification [6,7]. Furthermore, the recently mapped transcriptome-wide distributions of m⁶A in human and mouse cells indicate that this modification could affect a series

of biological processes including mRNA splicing, nuclear export, as well as host cellular immune response [8–10].

FTO and ALKBH5 belong to the AlkB family of iron(II)/ α -ketoglutarate(α -KG)-dependent dioxygenases [11,12]. Nine AlkB homologous have been identified in mammals: ALKBH1–8 and FTO, which show different preferences for substrates [13]. AlkB, ALKBH2, and ALKBH3 exhibit demethylation activity of 1-methyladenine (m¹A) and 3-methylcytosine (m³C) in DNA [14–16]. AlkB and ALKBH3 show higher activity to single-stranded (ss)DNA than double-stranded (ds)DNA, while ALKBH2 prefers dsDNA over ssDNA [16]. ALKBH8 contains an RNA recognition motif, a tRNA methyltransferase domain, and an AlkB-like domain, which could convert 5-carboxy-methyluridine (cm⁵U) to (S)-5-methoxycarbonyl-hydroxymethyluridine ((S)-mchm⁵U) [17,18]. FTO, a protein associated with human obesity [19–21], was originally shown to demethylate 3-methylthymine (m³T) in ssDNA and 3-methyluracil (m³U) in ssRNA [11,22]. Recently, our group discovered FTO as the first RNA demethylase that mediated demethylation of m⁶A to adenosine (A) [6]. Further research in our group indicated that FTO generated two intermediates (N⁶-hydroxymethyladenosine (hm⁶A) and N⁶-formyladenosine (fm⁶A)) during the demethylation process [23], which added potential complexity to this demethylation regulation [24].

Abbreviations: m⁶A, N⁶-methyladenosine; hm⁶A, N⁶-hydroxymethyladenosine; fm⁶A, N⁶-formyladenosine; A, adenosine; fALKBH5, zebrafish ALKBH5; α -KG, α -ketoglutarate; m¹A, 1-methyladenine; m³C, 3-methylcytosine; ss, single-stranded; ds, double-stranded; cm⁵U, 5-carboxy-methyluridine; (S)-mchm⁵U, (S)-5-methoxycarbonyl-hydroxymethyluridine; m³T, 3-methylthymine; m³U, 3-methyluracil; Δ fALKBH5, truncated zebrafish ALKBH5; IPTG, isopropyl β -D-1-thiogalactopyranoside; SIN, succinate acid; hALKBH3, human ALKBH3; hALKBH8, human ALKBH8; hALKBH2, human ALKBH2; rmsd, root-mean-square deviation

* Corresponding author. Fax: +1 773 702 0805.

E-mail address: chuanhe@uchicago.edu (C. He).

ALKBH5 is the second known m⁶A RNA demethylase *in vitro* and *in vivo* [7]. The over-expression of ALKBH5 leads to reduction of the cellular m⁶A level, while knockdown of ALKBH5 increases the ratio of m⁶A to A in mRNA in human cells and mouse testis [7]. Furthermore, aberrant spermatogenesis and apoptosis were observed in mouse testis when *Alkbh5* gene was knocked-out [7]. Although ALKBH5 and FTO exhibit similar substrate preference, their reaction pathways seem to be different: as we show in this study, ALKBH5 directly converts m⁶A to adenosine without any intermediate observed. Whereas, two intermediates of hm⁶A and fm⁶A are observed in the FTO-mediated m⁶A demethylation. Recently, the crystallization conditions for human ALKBH5 (hALKBH5) were published [25]; however, the structure has not been reported. Here we report the crystal structure of a truncated zebrafish ALKBH5 (Protein ID: NP_001070855, residues 38–287, named ΔfALKBH5 here and after), which shares high sequence identity to hALKBH5, as well as the same biological activity. This structure should facilitate our understanding of the substrate-selectivity of the AlkB family proteins, and provide further insights for future investigation into the mechanism of m⁶A demethylation.

2. Materials and methods

2.1. Cloning, expression, and purification

The truncated zebrafish ALKBH5 (ΔfALKBH5) gene was PCR-amplified from zebrafish cDNA (Thermo Scientific), and subcloned into PMCSG19 vector by ligation independent cloning (LIC) [26], resulting in the ΔfALKBH5-PMCSG19 plasmid with a His6-tag at N-terminal. The constructed plasmid was transformed in BL21 (DE3) strain containing PRK1037 plasmid [26]. Cells grew in LB medium containing 50 μg/mL kanamycin and 100 μg/mL Ampicillin at 37 °C. When OD₆₀₀ reached 0.6, the protein expression was achieved by adding 1 mM isopropyl β-D-1-thiogalactopyranoside (IPTG) under 16 °C for overnight. Cells were harvested and stored at –80 °C for subsequent steps.

The cell pellet was resuspended with 35 mL buffer A (10 mM Tris–HCl, pH 7.4, 500 mM NaCl and 1 mM DTT), and lysed by sonication. After centrifugation, the supernatant was loaded to pre-equilibrated Ni–NTA column and washed with eight column volumes of buffer A. Target protein was eluted with gradient linear buffer B (10 mM Tris–HCl, pH 7.4, 500 mM NaCl, 500 mM imidazole, and 1 mM DTT). After removing the His-tag by overnight TEV enzyme digestion at 4 °C, the protein solution was applied to MonoS column and eluted with linear concentration of NaCl in 10 mM Tris–HCl, pH 7.4. The eluted fractions were pooled, concentrated, and further purified by gel filtration Superdex200 column in 10 mM Tris–HCl, pH 7.4, 150 mM NaCl, and 1 mM DTT. Over 95% purity of protein was obtained for further use (Supplementary Fig. 1). FTO and hALKBH5 proteins were expressed and purified as reported [7,22].

2.2. Crystallization and data collection

The sitting-drop vapor diffusion method was employed for the crystallization of ΔfALKBH5/α-KG protein. 1 μL 10 mg/mL protein was mixed with an equal volume of reservoir solution (0.2 M sodium iodide, pH 7.0, 20% w/v polyethylene glycol 3,350) in the presence of 1 mM MnCl₂ and 2 mM α-KG, and equilibrated against 100 μL of the reservoir solution at 289 K. The crystals of ΔfALKBH5/succinate acid (SIN) were achieved under the same conditions except for the substitution of α-KG for succinate acid. The crystals appeared within 24 h and were flash-frozen in liquid nitrogen with 25% glycerol (v/v) as the cryoprotectant solution. The crystal

Table 1

Data collection and refinement statistics of ΔfALKBH5 in complex with α-KG or succinate acid (SIN).

	ΔfALKBH5/α-KG	ΔfALKBH5/SIN
<i>Data collection</i>		
Space group	P2 ₁ 2 ₁ 2 ₁	P2 ₁ 2 ₁ 2 ₁
Cell dimensions		
a, b, c (Å)	65.948, 68.595, 114.909	66.067, 69.792, 115.050
α, β, γ (°)	90.00, 90.00, 90.00	90.00, 90.00, 90.00
Resolution (Å)	30–1.65	50–1.80
R _{sym} or R _{merge}	8.9 (49.0)*	6.9 (59.4)
I/σ	27.8 (3.0)	22.5 (3.5)
Completeness (%)	96.1 (93.2)	99.9 (99.9)
Redundancy	5.7 (4.8)	6.4 (6.5)
<i>Refinement</i>		
Resolution (Å)	30–1.65 (1.71–1.65)	50–1.80 (1.86–1.80)
No. unique reflections	60,317	49,614
R _{work} /R _{free}	20.9/23.8	17.2/18.2
No. atoms		
Protein	3,406	3,370
Ligand/ion	22	18
Water	445	471
<i>B-factors</i>		
Protein	19.8	25.3
Ligand/ion	29.9	29.0
Water	30.1	37.2
<i>R.m.s. deviations</i>		
Bond lengths (Å)	0.007	0.009
Bond angles (°)	1.140	1.161

* Highest-resolution shell is shown in parentheses.

diffraction data was collected at the macromolecular crystallography for life science beamline NE-CAT (24-ID-D) at the Advanced Photon Source, Argonne National Laboratory. The data was then integrated and scaled with HKL2000 (Table 1).

2.3. Phasing and refinement

Zebrafish ALKBH5 structures were resolved by molecular replacement with the CCP4i program PHASER using the structure of *Escherichia coli* AlkB (PDB ID: 2FD8) as the searching model. The structure model building was performed using the computer graphics program Coot, and then refined by using Phenix. The final R/R_{free} factor value of ΔfALKBH5/α-KG and ΔfALKBH5/SIN is 20.9/23.8% and 17.2/18.2%, respectively (Table 1).

2.4. MADLI-TOF/TOF MS analysis

As reported previously [7], 1 nmol 9-mer ssRNA substrate (5'-UAAGm⁶ACUCA-3') was mixed with 1 nmol purified ΔfALKBH5/hALKBH5 protein in 100 μL reaction buffer (25 mM HEPES, pH 7.4, 100 mM KCl, 2 mM MgCl₂, 0.2 U/μL RNasin, 2 mM L-ascorbic acid, 300 μM α-KG and 150 μM (NH₄)₂Fe(SO₄)₂·6H₂O). After incubation at room temperature for 30 min, 10 μL reaction solution was mixed with 50 μL ion exchange resin (Bio-Rad). 1 μL solution was mixed with 1 μL matrix (THAP/Diammonium Citrate) and spotted onto MALDI plate. Then MALDI-TOF/TOF (Bruker) was employed to analyze the results.

2.5. HPLC analysis of ALKBH5 activity

100 μL reaction solution was quenched by 5 mM EDTA followed by heating at 95 °C for 10 min. The reacted ssRNA was digested with 1 μL nuclease P1 at 42 °C for overnight. Then 10 μL 1 M NH₄HCO₃ and 1 μL alkaline phosphatase were added to the solution and digested for 3 h at 37 °C. HPLC system equipped with an Acclaim 120, C18, 5 μm analytical column (Dionex, 059148) was

employed to analyze the result. 30 μ L digested solution was injected in HPLC and eluted with buffer A (50 mM ammonia acetate) and buffer B (60% acetonitrile, 0.01% TFA, 50 mM ammonia acetate) with a flow rate of 1 ml/min. The analysis was executed at room temperature. The detection wavelength was set at 260 nm.

3. Results and discussion

3.1. Sequence identity and biological activity of hALKBH5 and Δ fALKBH5

ALKBH5 shares high sequence identity among different species. Sequence alignment by ClustalW2 indicates that their differences are mainly distributed at the N- and C-termini with the active site highly conserved, including the five invariant residues (HxD...H...R...R) (Supplementary Fig. 2). After testing ALKBH5 from different species, we succeeded in crystallizing a truncated form of zebrafish ALKBH5 (Δ fALKBH5, residues 38–287) in complex with manganese(II) and α -KG. Full-length fALKBH5 shares 73.9% identity (260/352 residues) with hALKBH5, and the identity for Δ fALKBH5 reaches as high as 80.8% (202/250 residues).

To confirm that the truncation of fALKBH5 did not affect catalytic activity, a 9-mer ssRNA substrate (UAAGm⁶ACUCA) was treated with equal amounts of hALKBH5 and Δ fALKBH5 for 30 min at room temperature, respectively. MALDI-TOF/TOF was employed to analyze the results. A loss of 14 Da in substrate mass in experiments with both hALKBH5 and Δ fALKBH5 was observed, showing the m⁶A demethylation activity of Δ fALKBH5 (Fig. 1A). To further

confirm this observation, the reacted ssRNA was completely digested using nuclease P1 and alkaline phosphatase to single nucleosides, and then analyzed by HPLC. As shown in Fig. 1B, Δ fALKBH5 could completely demethylate m⁶A in the ssRNA substrate as hALKBH5.

3.2. The structure of Δ fALKBH5 and its active site

Δ fALKBH5 was crystallized in complex with manganese(II) and α -KG by mixing with an equal volume of reservoir solution (0.2 M sodium iodide, pH 7.0, 20% w/v polyethylene glycol 3,350) at 289 K, and a high-resolution (1.65 Å) X-ray diffraction data set was collected. *Escherichia coli* AlkB, the closest homologue of ALKBH5, shares 14.8% identity (37/250 residues) and 39.2% similarity (98/250 residues) with Δ fALKBH5. Using the structure of AlkB (PDB ID: 2FD8) as a searching model, the final model of Δ fALKBH5 structure was refined to 1.65 Å (Table 1). fALKBH5 is a monomer in solution, and there are two monomers per asymmetric unit in the P2₁2₁2₁ unit cell and they interact with each other mainly through a loop (named L2 here and after) (Supplementary Fig. 3). Δ fALKBH5 is composed of 11 β -strands and 3 long α -helices. As illustrated in Fig. 2, the active site of fALKBH5 is mainly composed of a jelly-roll motif [27], which is formed of eight β -strands (β 4– β 11). The β sheets are connected through loops and 3 α -helices buttress the jelly-roll motif from the outside.

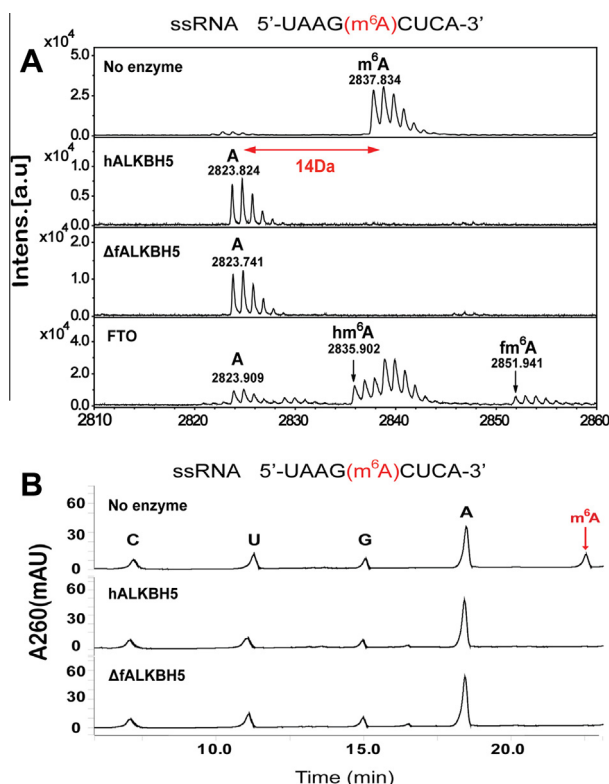


Fig. 1. (A) MALDI-TOF/TOF mass spectrometry analysis. hALKBH5 and Δ fALKBH5 showed the same activity of m⁶A demethylation on ssRNA (ssRNA 5'-UAAGm⁶ACUCA-3') with loss of 14-Dalton of a methyl group after the reaction in both cases. By contrast, after treating FTO with ssRNA, two intermediates hm⁶A (m⁶A-2 Da, lost a H₂O moiety during MALDI-TOF ionization) and fm⁶A (m⁶A + 14 Da) were observed. The two intermediates were not observed in the reactions with hALKBH5 and Δ fALKBH5 under the same condition. (B) HPLC chromatograms of digested nucleosides from m⁶A-containing ssRNA. HPLC confirmed the observation that after treatment with hALKBH5 and Δ fALKBH5, m⁶A underwent complete conversion to adenosine.

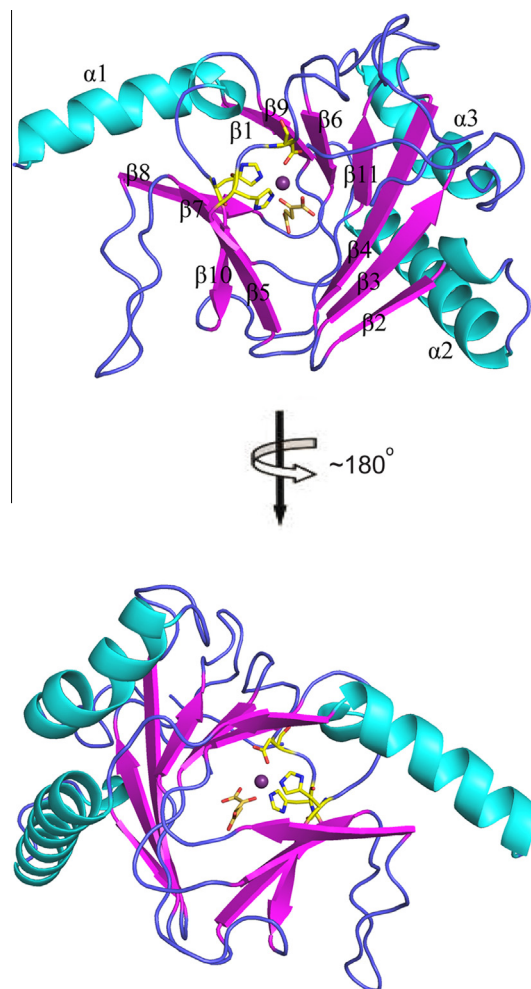


Fig. 2. The crystal structure of Δ fALKBH5. Two orthogonal views with catalytic core shown. The secondary structural elements are labeled α 1– α 3 for helices (colored cyan) and β 1– β 11 for strands (colored magenta).

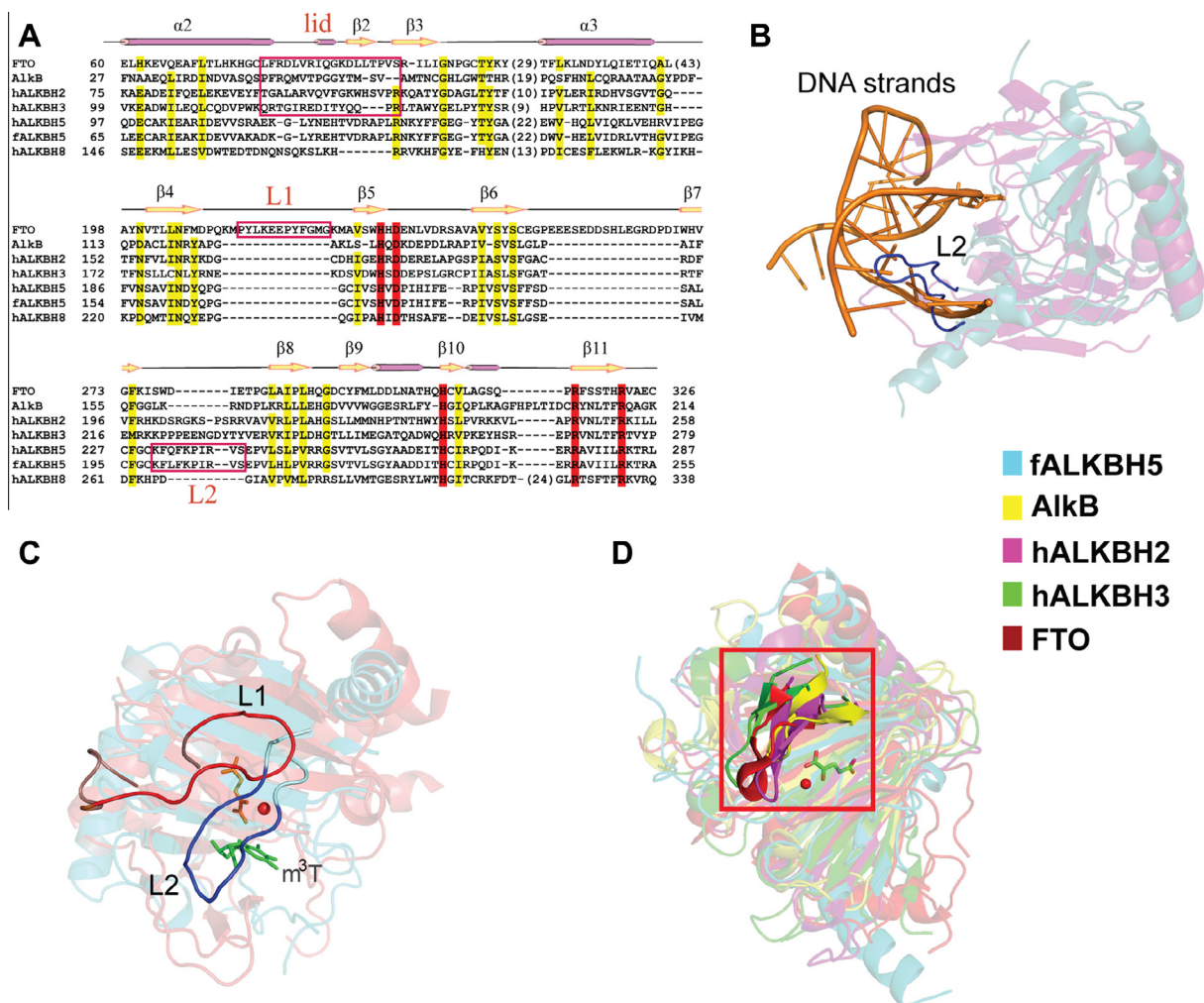


Fig. 3. The sequence and structure alignment of AlkB family members (FTO (PDB ID: 3LFM), hALKBH2 (PDB ID: 3BTX), hALKBH3 (PDB ID: 2IUW), AlkB (PDB ID: 2FD8), hALKBH8 and fALKBH5). (A) Structure-based sequence alignment of AlkB family proteins. The five invariant residues are highlighted in red. The loop L1 in FTO, L2 in human and fish ALKBH5 as well as the lid in FTO, hALKBH2, hALKBH3 and AlkB are boxed off in red. The secondary structure of fALKBH5 is shown on top of the alignment. (B) Structural comparison of fALKBH5 and hALKBH2-DNA. The L2 loop (colored in blue) in fALKBH5 protrudes into the dsDNA strand (colored in orange) from the superimposed hALKBH2-dsDNA structure. (C) Structure alignment of fALKBH5 and FTO with the extra loop highlighted. (L1 in FTO is colored red, and L2 in fALKBH5 is colored blue.) (D) A hairpin creates a lid over the active site in FTO, AlkB, hALKBH2 and hALKBH3. The structure of fALKBH5 lacks such a lid. The lid is highlighted in a red box.

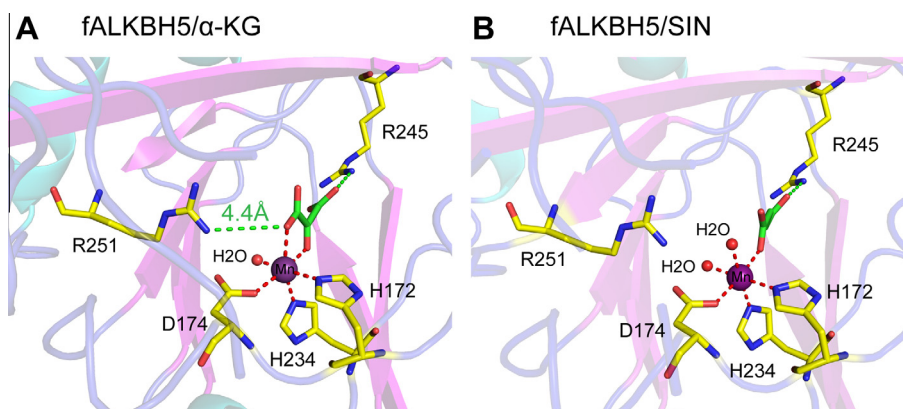


Fig. 4. The interaction network around Mn(II) and α-KG (A) or succinate (B). The coordinate bonds between Mn(II) and its ligands are shown with red dash lines, whereas the interactions between Arg245/Arg251 and α-KG/SIN are indicated in green. The distance between Arg251 and α-KG is 4.4 Å, indicating a weak interaction between them.

Sequence alignment shows that the consensus HxD...H...R...R residues in the active site of fALKBH5 are highly conserved (Fig. 3A and Supplementary Fig. 2), and structural alignment reveals five invariant residues reside in positions similar to those of other AlkB

family proteins (namely, human ALKBH2, hALKBH2; human ALKBH3, hALKBH3; human ALKBH8, hALKBH8; human FTO, FTO; and *Escherichia coli* AlkB, AlkB) (Supplementary Fig. 4). The root-mean-square deviation (rmsd) between fALKBH5 and its homo-

logues is within 3.5 Å (AlkB: 2.46 Å, hALKBH2: 2.62 Å, hALKBH3: 2.61 Å, hALKBH8: 1.75 Å, FTO: 3.16 Å). As showed in Fig. 4A and Supplementary Fig. 5, His172, Asp174, and His234 coordinate to manganese(II), and Arg245 interacts with α -KG through a salt bridge. It is noteworthy that the distance between Arg251 (the second arginine in the motif) and α -KG is 4.4 Å, whereas in other AlkB family proteins the corresponding residues are much closer to α -KG with the distance around 3 Å (Fig. 4A and Supplementary Fig. 6) [28–31]. This observation therefore suggests that Arg251 in Δ fALKBH5 may not bind α -KG, which differs from its equivalents in other AlkB homologous. Previous studies have confirmed that the (HxD...H...R...R) motif is highly conserved in all AlkB family members, and the five invariant residues are essential for enzymatic activity [32]. Usually, the second arginine is considered as an α -KG-binding residue, but our structure of Δ fALKBH5 shows a potential weaker interaction between Arg251 and α -KG.

α -KG is the cofactor for the oxidation reaction catalyzed by ALKBH5, in which it is converted to succinic acid [13]. The addition of α -KG or succinic acid could help stabilize fALKBH5 protein and thus facilitates its crystallization. We also obtained the structure of Δ fALKBH5 in complex with manganese(II) and succinic acid at 1.80 Å resolution (Table 1). In both structures, the manganese(II) adopts a hexa-coordination geometry. Besides the three ligand residues (His172, Asp174, and His234) from the protein, two water molecules and succinate occupy the three remaining coordinate sites of the central manganese(II) in this succinate-bound form (Fig. 4B), while one water and two oxygen from α -KG bind the metal in the α -KG-bound form (Fig. 4A).

3.3. Structure and sequence comparison with other AlkB family proteins

An overlap of the current structure with the structure of hALKBH2-dsDNA [33] yielded some interesting observations. We found that the loop L2 in Δ fALKBH5 protruded into the dsDNA strand in the overlapped hALKBH2-dsDNA structure (Fig. 3B). ALKBH5 has been shown to exhibit much higher activity to ssRNA than dsRNA [7]; this L2 loop most likely plays the role of discriminating against duplex nucleic acids. In addition, the basic residues in the loop are prone to form hydrogen bonds with acidic residues, which may act to enhance the binding of fALKBH5 to ssRNA. It is interesting that FTO also has a loop (referred as L1) that clashes

with potential duplex nucleic acid substrates [30]. The sequence alignment shows that the L1 loop in FTO is unique among the AlkB family proteins (Fig. 3A). The L2 loop is highly conserved among ALKBH5 in different species, and has no similarity to other AlkB family proteins as well (Fig. 3A and Supplementary Fig. 2). An overlay of the structure of FTO and fALKBH5 revealed further insights. We found that L1 and L2 loops are both close to the active site. However, the two loops extend from the opposite directions (Fig. 3C). The two loops most likely play similar roles in blocking potential dsDNA/RNA from gaining access to the substrate-binding site. In addition, Δ fALKBH5 lacks a lid composed of two β -strands over the active site, which exists in FTO as well as in AlkB, hALKBH2, and hALKBH3 (Fig. 3A and D). Referred as “nucleotide recognition lid” in AlkB, this lid is conformationally flexible and is involved in binding to nucleotide substrates. It has been proposed to play a role in the substrate recognition [31]. hALKBH2, hALKBH3 and FTO also possess similar lids that are assumed to perform the same function [28,30,33]. However, this lid is not conserved among other these proteins in the AlkB family (Fig. 3A). Comparing the structures of fALKBH5 and FTO, the lid in FTO covers the active site while its absence in fALKBH5 makes the active site more exposed (Supplementary Fig. 7).

3.4. Residues comparison near active site between FTO and fALKBH5

Among all AlkB family proteins, we are most interested in comparisons between ALKBH5 and another m⁶A demethylase, FTO. We first assayed the demethylation of hALKBH5 with m⁶A-containing RNA. Under the same conditions that we were able to observe hm⁶A and fm⁶A intermediates in the FTO-mediated m⁶A oxidation, we failed to observe these intermediates in the reaction with hALKBH5 and fALKBH5 (Fig. 1A). This observation suggests that ALKBH5 might go through a mechanism of m⁶A demethylation slightly different from FTO. Supplementary Fig. 8 illustrates the proposed m⁶A demethylation process. FTO could generate intermediates of hm⁶A and fm⁶A in a step-wise manner when converting m⁶A to A, and both hm⁶A and fm⁶A would decompose to adenosine in aqueous solution with both half-lives of around 3 h [23]. By contrast, ALKBH5 demethylates m⁶A to A without observing these intermediates. It is possible that ALKBH5 facilitates/catalyzes decomposition of the generated hm⁶A when bound to the active site. The exact mechanistic difference related to the production of hm⁶A will need further biochemical and computational investigations in the future. As viewed through structural alignment, most of residues are visibly conserved except Lys100, Ile169, and Pro175 between fALKBH5 and FTO, which correspond with Arg96, Val228 and Glu234 in FTO (Fig. 5). These three residues in ALKBH5 are also highly conserved among different species (Supplementary Fig. 2). As neutral and hydrophobic residues, Ile169 and Val228 may not directly participate in the demethylation process. Glu234 was reported to form a hydrogen bond with m³T in the FTO-m³T structure, and the mutation of Glu234 to proline resulted in the loss of FTO activity of demethylating m³T [30]. As illustrated in Fig. 5, Pro175 lies in the corresponding position in fALKBH5, which could not form the similar hydrogen bond with nucleic substrates. In addition, mutation of Arg96 in FTO to methionine, glutamine or histidine leads to loss of FTO demethylation activity [30,34], while its equivalent residue is Lys100 in fALKBH5. We have mutated Lys100 to arginine and Pro175 to glutamic acid in fALKBH5, respectively, and tested the demethylation activity of both mutant proteins by MALDI-TOF. As showed in Supplementary Fig. 9, a reduced m⁶A demethylation activity was observed for Δ fALKBH5 P175E, whereas Δ fALKBH5 K100R almost lost its activity. This result indicates that Lys100 and Pro175 in fALKBH5 are involved in m⁶A demethylation. Future mechanistic studies are required to study differences between ALKBH5 and FTO.

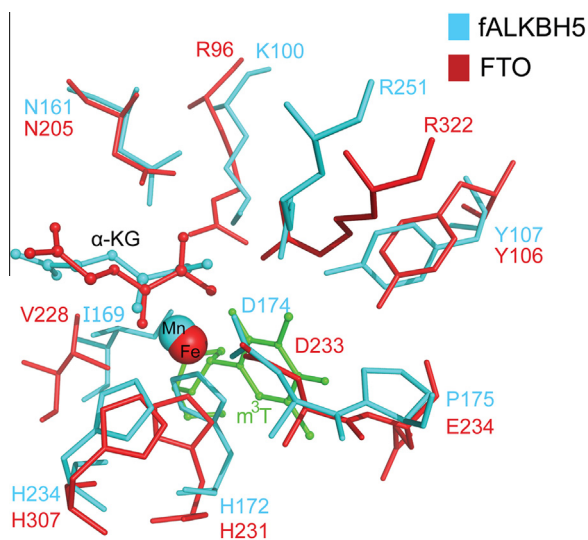


Fig. 5. Superimposition of residues near the catalytic core in fALKBH5 and FTO. The mononucleotide m³T in FTO is colored green, residues in fALKBH5 and FTO are labeled in cyan and red, respectively.

4. Conclusions

The non-heme α -KG-dependent AlkB family demethylases mainly catalyze the oxidative demethylation of *N*-alkylated nucleic acid bases. These members possess a similar catalytic core as well as a highly conserved (HxD...H...R...R) motif. Their substrates differ, however. The molecular basis of substrate-selection and reactions mechanisms have attracted much research attention. Here, we present the high resolution structure of FALK-BH5 at 1.65 Å. FTO possesses a loop (L1) that is important for ssRNA-binding, while FALKBH5 possesses a different loop (L2) extended from the opposite direction to accomplish the same function. The presence of this loop explains the preference of ALKBH5 for ssRNA. We also show that unlike FTO, which generates hm⁶A and fm⁶A as intermediates in the process of m⁶A demethylation, such intermediates are not observed in demethylation reactions catalyzed by ALKBH5. Differences in active residues between these two proteins, as well as the weaker interaction between Arg251 and α -KG may explain the slight difference in the demethylation pathways of these two proteins. In summary, we report the structure of FALKBH5, which provides a molecular basis for the study of substrate-selection specificity in the AlkB family. With this structure now available, future work will focus on elucidating the potential mechanistic differences between FTO and ALKBH5 m⁶A demethylation and the potential impact to biology functions.

5. PDB references

Δ fALKBH5/ α -KG 4NPL and Δ fALKBH5/SIN 4NPM.

Acknowledgements

We thank Dr. Kay Perry from NE-CAT for structure data processing and structure determination. S.F. Reichard, MA contributed editing. This work is supported by National Institutes of Health GM071440 (to C.H.). W.C. was partially supported by the China Scholar Program, the National Nature Science Foundation of China (91013009 and 21071077) and the Ministry of Science and Technology of China Key Project (2012CB933802).

Appendix A. Supplementary data

Supplementary data associated with this article can be found, in the online version, at <http://dx.doi.org/10.1016/j.febslet.2014.02.021>.

References

- [1] Bokar, J.A. (2005) The biosynthesis and functional roles of methylated nucleosides in eukaryotic mRNA. *Fine-tuning of RNA functions by modification and editing, topics in current genetics*, 12, pp. 141–177, Springer.
- [2] Beemon, K. and Keith, J. (1977) Localization of N⁶-methyladenosine in the rous sarcoma virus genome. *J. Mol. Biol.* 113, 165–179.
- [3] Shah, J. and Clancy, M. (1992) IME4, a gene that mediates MAT and nutritional control of meiosis in *Saccharomyces cerevisiae*. *Mol. Cell Biol.* 12, 1078–1086.
- [4] Bodi, Z., Zhong, S., Mehra, S., Song, J., Graham, N., Li, H., May, S. and Fray, R.G. (2012) Adenosine methylation in *Arabidopsis* mRNA is associated with the 3' end and reduced levels cause developmental defects. *Front. Plant Sci.* 48, 1–9.
- [5] Bokar, J., Shambaugh, M., Polayes, D., Matera, A. and Rottman, F. (1997) Purification and cDNA cloning of the AdoMet-binding subunit of the human mRNA (N⁶-adenosine)-methyltransferase. *RNA* 3, 1233–1247.
- [6] Jia, G., Fu, Y., Zhao, X., Dai, Q., Zheng, G., Yang, Y., Yi, C., Lindahl, T., Pan, T., Yang, Y.G. and He, C. (2011) N⁶-methyladenosine in nuclear RNA is a major substrate of the obesity-associated FTO. *Nat. Chem. Biol.* 7, 885–887.
- [7] Zheng, G., Dahl, J.A., Niu, Y., Fedorcsak, P., Huang, C.M., Li, C.J., Vågbo, C.B., Shi, Y., Wang, W.L., Song, S.H., Lu, Z., Bosmans, R.P.G., Dai, Q., Hao, Y.J., Yang, X., Zhao, W.M., Tong, W.M., Wang, X.J., Bogdan, F., Furu, K., Fu, Y., Jia, G., Zhao, X., Liu, J., Krokan, H.E., Klungland, A., Yang, Y.G. and He, C. (2012) ALKBH5 is a mammalian RNA demethylase that impacts RNA metabolism and mouse fertility. *Mol. Cell* 49, 18–29.
- [8] Dominissini, D., Moshitch-Moshkovitz, S., Schwartz, S., Salmon-Divon, M., Ungar, L., Osenberg, S., Cesarkas, K., Jacob-Hirsch, J., Amariglio, N., Kupiec, M., Sorek, R. and Rechavi, G. (2012) Topology of the human and mouse m⁶A RNA methylomes revealed by m⁶A-seq. *Nature* 485, 201–206.
- [9] Meyer, K.D., Saletore, Y., Zumbo, P., Elemento, O., Mason, C.E. and Jaffrey, S.R. (2012) Comprehensive analysis of mRNA methylation reveals enrichment in 3' UTRs and near stop codons. *Cell* 149, 1635–1646.
- [10] Karikó, K., Buckstein, M., Ni, H. and Weissman, D. (2005) Suppression of RNA recognition by Toll-like receptors: the impact of nucleoside modification and the evolutionary origin of RNA. *Immunity* 23, 165–175.
- [11] Gerken, T., Girard, C.A., Tung, Y.C.L., Webby, C.J., Saudek, V., Hewitson, K.S., Yeo, G.S., McDonough, M.A., Cunliffe, S., McNeill, L.A., Galvanovskis, J., Rorsman, P., Robins, P., Prieur, X., Coll, A.P., Ma, M., Jovanovic, Z., Farooqi, I.S., Sedgwick, B., Barroso, I., Lindahl, T., Ponting, C.P., Ashcroft, F.M., O'Rahilly, S. and Schofield, C.J. (2007) The obesity-associated FTO gene encodes a 2-oxoglutarate-dependent nucleic acid demethylase. *Science* 318, 1469–1472.
- [12] Kurowski, M.A., Bhagwat, A.S., Papaj, G. and Bujnicki, J.M. (2003) Phylogenomic identification of five new human homologs of the DNA repair enzyme AlkB. *BMC Genomics* 4, 48.
- [13] Yi, C., Yang, C.G. and He, C. (2009) A non-heme iron-mediated chemical demethylation in DNA and RNA. *Acc. Chem. Res.* 42, 519–529.
- [14] Treweek, S.C., Henshaw, T.F., Hausinger, R.P., Lindahl, T. and Sedgwick, B. (2002) Oxidative demethylation by *Escherichia coli* AlkB directly reverses DNA base damage. *Nature* 419, 174–178.
- [15] Falnes, P.O., Johansen, R.F. and Seeberg, E. (2002) AlkB-mediated oxidative demethylation reverses DNA damage in *Escherichia coli*. *Nature* 419, 178–182.
- [16] Aas, P.A., Otterlei, M., Falnes, P.O., Vågbo, C.B., Skorpen, F., Akbari, M., Sundheim, O., Björås, M., Slupphaug, G., Seeberg, E. and Krokan, H.E. (2003) Human and bacterial oxidative demethylases repair alkylation damage in both RNA and DNA. *Nature* 421, 859–863.
- [17] Fu, Y., Dai, Q., Zhang, W., Ren, J., Pan, T. and He, C. (2010) The AlkB Domain of Mammalian ABH8 Catalyzes Hydroxylation of 5-Methoxycarbonylmethyluridine at the Wobble Position of tRNA. *Angew. Chem., Int. Ed.* 49, 8885–8888.
- [18] van den Born, E., Vågbo, C.B., Songe-Møller, L., Leihne, V., Lien, G.F., Leszczynska, G., Malkiewicz, A., Krokan, H.E., Kirpekar, F., Klungland, A. and Falnes, P.O. (2011) ALKBH8-mediated formation of a novel diastereomeric pair of wobble nucleosides in mammalian tRNA. *Nat. Commun.* 2, 172.
- [19] Dina, C., Meyre, D., Gallina, S., Durand, E., Körner, A., Jacobson, P., Carlsson, L.M., Kiess, W., Vatin, V., Lecocq, C., Delplanque, J., Vaillant, E., Pattou, F., Ruiz, J., Weill, J., Levy-Marchal, C., Horber, F., Potoczna, N., Hercberg, S., Stunff, C.L., Bougnères, P., Kovacs, P., Marre, M., Balkau, B., Cauchi, S.P., Chèvre, J.C. and Froguel, P. (2007) Variation in FTO contributes to childhood obesity and severe adult obesity. *Nat. Genet.* 39, 724–726.
- [20] Frayling, T.M., Timpson, N.J., Weedon, M.N., Zeggini, E., Freathy, R.M., Lindgren, C.M., Perry, J.R., Elliott, K.S., Lango, H., Rayner, N.W., Shield, B., Harries, L.W., Barrett, J.C., Ellard, S., Groves, C.J., Knight, B., Patch, A.M., Ness, A.R., Ebrahim, S., Lawlor, D.A., Ring, S.M., Ben-Shlomo, Y., Jarvelin, M.R., Sovio, U., Bennett, A.J., Melzer, D., Ferrucci, L., Loos, R.J.F., Barroso, I., Wareham, N.J., Karpe, F., Owen, K.R., Cardon, L.R., Walker, M., Hitman, G.A., Palmer, C.N.A., Doney, A.S.F., Morris, A.D., Smith, G.D., Hattersley, A.T. and McCarthy, M.I. (2007) A common variant in the FTO gene is associated with body mass index and predisposes to childhood and adult obesity. *Science* 316, 889–894.
- [21] Scuteri, A., Sanna, S., Chen, W.M., Uda, M., Albai, G., Strait, J., Najjar, S., Nagaraja, R., Orrù, M., Usala, G., Dei, M., Lai, S., Maschio, A., Busonero, F., Mulas, A., Ehret, G.B., Fink, A.A., Weder, A.B., Cooper, R.S., Galan, P., Chakravarti, A., Schlessinger, D., Cao, A., Lakatta, E. and Abecasis, G.R. (2007) Genome-wide association scan shows genetic variants in the FTO gene are associated with obesity-related traits. *PLoS Genet.* 3, e115.
- [22] Jia, G., Yang, C.G., Yang, S., Jian, X., Yi, C., Zhou, Z. and He, C. (2008) Oxidative demethylation of 3-methylthymine and 3-methyluracil in single-stranded DNA and RNA by mouse and human FTO. *FEBS Lett.* 582, 3313–3319.
- [23] Fu, Y., Jia, G., Pang, X., Wang, R.N., Wang, X., Li, C.J., Smemo, S., Dai, Q., Bailey, K.A., Nobrega, M.A., Han, K.L., Cui, Q. and He, C. (2013) FTO-mediated formation of N⁶-hydroxymethyladenosine and N⁶-formyladenosine in mammalian RNA. *Nat. Commun.* 4, 1798.
- [24] He, C. (2010) Grand challenge commentary: RNA epigenetics? *Nat. Chem. Biol.* 6, 863–865.
- [25] Zhou, B. and Han, Z. (2013) Crystallization and preliminary X-ray diffraction of the RNA demethylase ALKBH5. *Acta Crystallogr. F* 69, 1231–1234.
- [26] Donnelly, M.I., Zhou, M., Millard, C.S., Clancy, S., Stols, L., Eschenfeldt, W.H., Collart, F.R. and Joachimiak, A. (2006) An expression vector tailored for large-scale, high-throughput purification of recombinant proteins. *Protein Expression. Purif.* 47, 446–454.
- [27] Costas, M., Mehn, M.P., Jensen, M.P. and Que, L. (2004) Dioxygen activation at mononuclear nonheme iron active sites: enzymes, models, and intermediates. *Chem. Rev.* 104, 939–986.
- [28] Sundheim, O., Vågbo, C.B., Björås, M., Sousa, M.M., Talstad, V., Aas, P.A., Drablos, F., Krokan, H.E., Tainer, J.A. and Slupphaug, G. (2006) Human ABH3 structure and key residues for oxidative demethylation to reverse DNA/RNA damage. *EMBO J.* 25, 3389–3397.
- [29] Pastore, C., Topalidou, I., Forouhar, F., Yan, A.C., Levy, M. and Hunt, J.F. (2012) Crystal structure and RNA binding properties of the RNA recognition motif

- (RRM) and AlkB domains in human AlkB homolog 8 (ABH8), an enzyme catalyzing tRNA hypermodification. *J. Biol. Chem.* 287, 2130–2143.
- [30] Han, Z., Niu, T., Chang, J., Lei, X., Zhao, M., Wang, Q., Cheng, W., Wang, J., Feng, Y. and Chai, J. (2010) Crystal structure of the FTO protein reveals basis for its substrate specificity. *Nature* 464, 1205–1209.
- [31] Yu, B., Edstrom, W.C., Benach, J., Hamuro, Y., Weber, P.C., Gibney, B.R. and Hunt, J.F. (2006) Crystal structures of catalytic complexes of the oxidative DNA/RNA repair enzyme AlkB. *Nature* 439, 879–884.
- [32] Mishina, Y., Duguid, E.M. and He, C. (2006) Direct reversal of DNA alkylation damage. *Chem. Rev.* 106, 215–232.
- [33] Yang, C.G., Yi, C., Duguid, E.M., Sullivan, C.T., Jian, X., Rice, P.A. and He, C. (2008) Crystal structures of DNA/RNA repair enzymes AlkB and ABH2 bound to dsDNA. *Nature* 452, 961–965.
- [34] Meyre, D., Proulx, K., Kawagoe-Takaki, H., Vatin, V., Gutiérrez-Aguilar, R., Lyon, D., Ma, M., Choquet, H., Horber, F., Van Hul, W., Van Gaal, L., Balkau, B., Pattou, F.O., Farooqi, I.S., Saudek, V., O'Rahilly, S., Froguel, P., Sedgwick, B. and Yeo, G.S. (2010) Prevalence of loss-of-function FTO mutations in lean and obese individuals. *Diabetes* 59, 311–318.